

Crystal structure of a complete ternary complex of T-cell receptor, peptide–MHC, and CD4

Yiyuan Yin^{a,b,1,2}, Xin Xiang Wang^{a,c,1}, and Roy A. Mariuzza^{a,c,3}

^aW. M. Keck Laboratory for Structural Biology, Institute for Bioscience and Biotechnology Research, University of Maryland, Rockville, MD 20850; and ^bProgram in Molecular and Cell Biology and ^cDepartment of Cell Biology and Molecular Genetics, University of Maryland, College Park, MD 20742

Edited* by Stanley G. Nathenson, Albert Einstein College of Medicine, Bronx, NY, and approved February 27, 2012 (received for review December 6, 2011)

Adaptive immunity depends on specific recognition by a T-cell receptor (TCR) of an antigenic peptide bound to a major histocompatibility complex (pMHC) molecule on an antigen-presenting cell (APC). In addition, T-cell activation generally requires binding of this same pMHC to a CD4 or CD8 coreceptor. Here, we report the structure of a complete TCR–pMHC–CD4 ternary complex involving a human autoimmune TCR, a myelin-derived self-peptide bound to HLA-DR4, and CD4. The complex resembles a pointed arch in which TCR and CD4 are each tilted ~65° relative to the T-cell membrane. By precluding direct contacts between TCR and CD4, the structure explains how TCR and CD4 on the T cell can simultaneously, yet independently, engage the same pMHC on the APC. The structure, in conjunction with previous mutagenesis data, places TCR-associated CD3 $\epsilon\gamma$ and CD3 $\epsilon\delta$ subunits, which transmit activation signals to the T cell, inside the TCR–pMHC–CD4 arch, facing CD4. By establishing anchor points for TCR and CD4 on the T-cell membrane, the complex provides a basis for understanding how the CD4 coreceptor focuses TCR on MHC to guide TCR docking on pMHC during thymic T-cell selection.

T-cell receptors (TCRs) recognize peptides presented by major histocompatibility complex molecules (pMHC) to discriminate foreign from self-antigens and trigger adaptive immune responses. In addition, T-cell signaling is enhanced by the coreceptors CD4 and CD8, which are expressed on T-helper cells and cytotoxic T lymphocytes, respectively (1). These transmembrane glycoproteins bind MHC class II (CD4) or MHC class I (CD8) molecules on the surface of antigen-presenting cells (APCs). The interaction of CD4 with MHC class II greatly increases cytokine production by helper T cells (1) and substantially reduces the number of antigenic peptides on APCs required for T-cell triggering (2). Similarly, the CD8–MHC class I interaction augments the sensitivity and response of cytotoxic T cells to pMHC ligands (3).

It is generally believed that the main function of the CD4 and CD8 coreceptors is to recruit the Src tyrosine kinase Lck to the TCR–pMHC complex upon coreceptor binding to MHC, leading to formation of a TCR–pMHC–CD4 or TCR–pMHC–CD8 ternary complex (4–8). Recruitment of Lck, which occurs via its association with the cytoplasmic tail of CD4 or CD8, promotes phosphorylation of immunoreceptor tyrosine activation motifs (ITAMs) in the cytoplasmic tails of CD3 subunits associated with the TCR, resulting in signal amplification.

Although numerous (>25) structures of TCR–pMHC binary complexes have been determined (9–11), no structure of a TCR–pMHC–CD4 or TCR–pMHC–CD8 ternary complex has been reported. A hypothetical model of the TCR–pMHC–CD4 complex has been constructed that would rule out direct interactions between CD4 and TCR (12), which seemingly contradicts certain functional and biochemical evidence that CD4 physically associates with TCR (13). One possibility is that CD4 and TCR associate indirectly through other proteins, in particular CD3. Another is that CD4 bridges TCRs interacting with agonist pMHC and endogenous pMHC complexes, creating a TCR “pseudodimer” capable of intracellular signaling (14). A third possibility is that CD4, which consists of four Ig-like domains

(D1–D4), possesses a greater degree of segmental flexibility than implied by the CD4 D1–D4 crystal structure (15). In this regard, small angle X-ray scattering (SAXS) has provided evidence that CD4 undergoes a large conformational rearrangement at the D2–D3 junction upon binding the HIV viral entry protein gp120 (16). Clearly, a structure of CD4 D1–D4 bound to TCR–pMHC is critical to resolving this issue.

There is considerable controversy over the mechanism of TCR triggering, and a variety of models have been proposed to explain how the TCR transduces signals across the T-cell membrane after binding pMHC (17). Some of these models evoke dimerization or oligomerization of CD4 (15), MHC (18), or TCR (19) as a means of enhancing phosphorylation of CD3 ITAMs by increasing the proximity of associated tyrosine kinases. However, the plausibility of these models must be assessed in terms of the geometrical constraints that would be imposed by a TCR–pMHC–CD4 structure.

Much effort has been directed at explaining the remarkably conserved diagonal binding mode observed in TCR–pMHC complexes (9, 10). This has been hypothesized to result from a genetically encoded bias of TCRs toward MHC (10, 20–22) and/or the need for the CD4 or CD8 coreceptor for T-cell development and efficient signaling (22–25). Whereas the search for evolutionarily conserved interactions between TCR and MHC molecules has benefited from the wealth of X-ray crystallographic information on TCR–pMHC binary complexes (9–11), a structural framework for understanding how CD4 or CD8 could restrict TCR docking options on pMHC has been lacking. The TCR–pMHC–CD4 ternary complex described here, comprising a human autoimmune TCR, HLA-DR4, and CD4 D1–D4, provides such a framework.

Results and Discussion

Structure Determination. A major obstacle to crystallizing a TCR–pMHC–CD4 ternary complex is its intrinsic instability, attributable to the low affinities of the binary interactions. Indeed, the affinity of the pMHC–CD4 interaction, the dissociation constant (K_D) of which has been variously estimated to range from ~200 μ M to >2 mM (13, 26), is even weaker than that of most TCR–pMHC interactions (1–100 μ M) (13). To overcome this difficulty, we used in vitro-directed evolution by yeast surface

Author contributions: Y.Y., X.X.W., and R.A.M. designed research; Y.Y. and X.X.W. performed research; Y.Y., X.X.W., and R.A.M. analyzed data; and Y.Y. and R.A.M. wrote the paper.

The authors declare no conflict of interest.

*This Direct Submission article had a prearranged editor.

Data deposition: The crystallography, atomic coordinates, and structure factors reported in this paper have been deposited in the Protein Data Bank, www.pdb.org (PDB ID code 3TOE).

¹Y.Y. and X.X.W. contributed equally to this work.

²Present address: Department of Antibody Engineering, Genentech, South San Francisco, CA 94080.

³To whom correspondence should be addressed. E-mail: rmariuzz@umd.edu.

This article contains supporting information online at www.pnas.org/lookup/suppl/doi:10.1073/pnas.1118801109/-DCSupplemental.

display to increase the affinity of human CD4 for the MHC class II molecule HLA-DR1 (27). We subjected the CD4 D1 domain to in vitro random mutagenesis, and displayed the resulting mutant CD4 library on the yeast surface by fusion to agglutinin protein Aga2p. The library was sorted by flow cytometry with HLA-DR1 to isolate CD4 variants with increased affinity. One of these variants, which contains two substitutions in CD4 D1 (Gln40Tyr/Thr45Trp), was produced as a full-length ectodomain (CD4 D1–D4) by secretion from baculovirus-infected insect cells. This CD4 mutant bound HLA-DR1 with $K_D = 8.8 \mu\text{M}$, compared with no detectable binding for wild-type CD4, even at concentrations up to $400 \mu\text{M}$ (27). The CD4 mutant exhibited similar affinity for HLA-DR4 ($K_D = 10.1 \mu\text{M}$), as measured by surface plasmon resonance (SPR) (Fig. 1). Therefore, it was used for cocrystallization with HLA-DR4 bearing a self-peptide from myelin basic protein (MBP) and the human autoimmune TCR MS2-3C8. We previously showed that MS2-3C8 engages its ligand via the canonical docking mode of $\alpha\beta$ TCRs (28), in which the TCR adopts a central diagonal orientation over pMHC (9, 10). The affinity of MS2-3C8 for MBP–DR4 is $5 \mu\text{M}$ (28), which is at the high end of the range for TCR–pMHC interactions (13).

Remarkably, the MS2-3C8–MBP–DR4–CD4 complex crystallized spontaneously from an equimolar mixture of the three proteins, without the aid of precipitants. The structure was determined to $4.0\text{-}\text{\AA}$ resolution by molecular replacement using the MS2-3C8–MBP–DR4 complex (28) and CD4 (15) as search models (Fig. 2A). The final R_{work} and R_{free} values are 23.8% and 30.5%, respectively (Table S1). Despite the modest resolution, the electron density was interpretable throughout, and the maps were of sufficient quality to unambiguously assemble the entire TCR–pMHC–CD4 complex (Fig. 2B). Moreover, electron density was visible for carbohydrates attached to CD4 residues Asn271 and Asn300 in domains D3 and D4, respectively, the only two *N*-linked glycosylation sites in human CD4.

Overview of the TCR–pMHC–CD4 Complex. The TCR–pMHC–CD4 complex resembles a pointed arch in which both TCR and CD4 are tilted rather than oriented vertically (Fig. 2A). The apex of the arch is formed by the $\alpha 2$ and $\beta 2$ domains of HLA-DR4 and the D1 domain of CD4. In this view, the complex is oriented as if the TCR and CD4 molecules stand on the T-cell surface at the bottom where they reach up to engage the MHC class II molecule on an opposing APC above. The TCR makes an angle of $\sim 60^\circ$ with the T-cell surface and the CD4 molecule an angle of

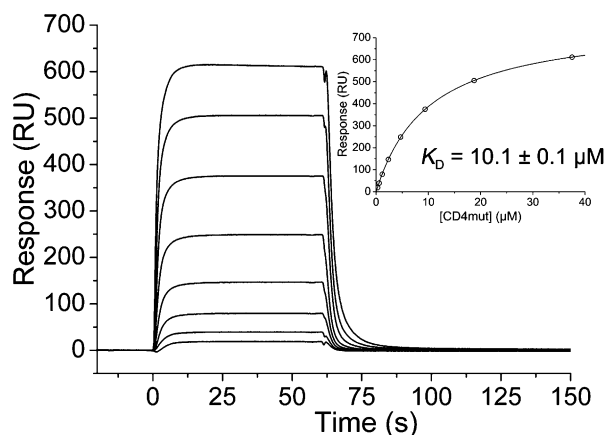


Fig. 1. SPR analysis of the binding of affinity-matured human CD4 mutant to HLA-DR4. SPR sensorgrams for the interaction of the CD4 mutant (0.3, 0.6, 1.2, 2.3, 4.7, 9.4, 18.8, and $37.5 \mu\text{M}$) with immobilized HLA-DR4 (1,600 resonance units). *Inset* shows fitting curve for equilibrium binding that resulted in a K_D of $10.1 \pm 0.1 \mu\text{M}$.

$\sim 70^\circ$; the apical angle between pMHC and CD4 is $\sim 50^\circ$ (Fig. 2A).

Importantly, superposition of the pMHC–CD4 D1–D2 portion of the MS2-3C8–MBP–DR4–CD4 structure onto the complex between mouse I-A^k and wild-type human CD4 D1–D2 (12) gave a root mean squared (r.m.s.) difference of 1.6\AA for 465 α -carbon atoms, indicating that affinity maturation of CD4 did not affect its overall binding mode to MHC class II. In both cases, CD4 engages MHC class II through its membrane-distal D1 domain at a concavity formed by the MHC $\alpha 2$ and $\beta 2$ domains (Fig. 2A). As we showed previously (27), the Gln40Tyr/Thr45Trp substitutions in affinity-matured CD4 improved shape complementarity and increased hydrophobic interactions at the interface with MHC class II through minor adjustments at the mutation sites, without altering overall complex orientation. Moreover, all CD4-contacting residues are invariant across human HLA-DR, -DP, and -DQ alleles and nearly invariant across mouse I-A and I-E alleles (27). Therefore, the topology of the CD4–MHC class II interaction observed in MS2-3C8–MBP–DR4–CD4 structure is

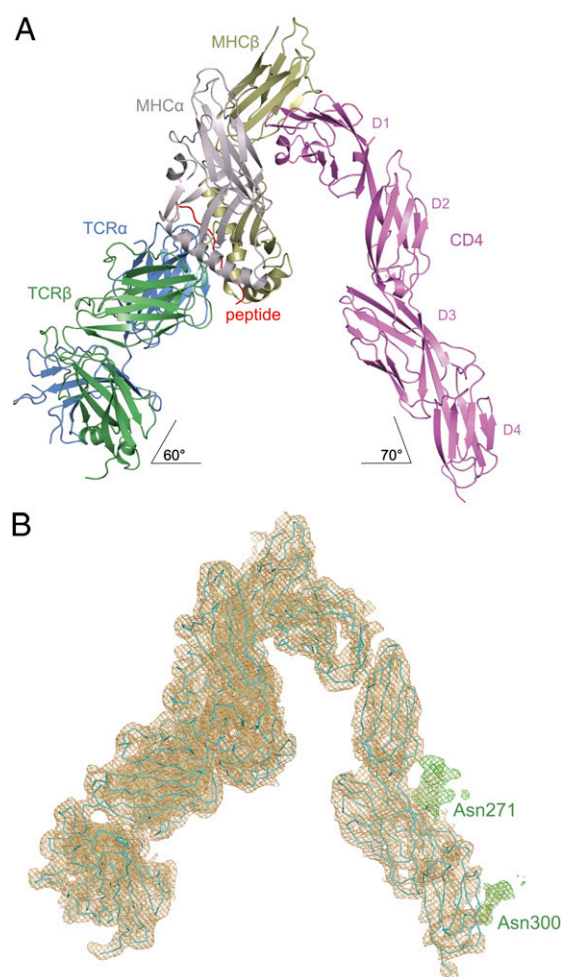


Fig. 2. Overview of the TCR–pMHC–CD4 ternary complex. (A) Ribbon diagram of the complex oriented as if the TCR MS2-3C8 and CD4 molecules are attached to the T cell at the bottom and the HLA-DR4 MHC class II molecule is attached to an opposing APC at the top. TCR α chain, blue; TCR β chain, green; CD4, pink; MHC α chain, gray; MHC β chain, yellow; MBP peptide, red. (B) σ_A -weighted $2F_o - F_c$ electron density map of the complete TCR–pMHC–CD4 complex (contoured at 1σ). The orientation is the same as in A. In green is electron density for carbohydrates attached to CD4 Asn271 and Asn300 in domains D3 and D4, respectively. Protein molecules are shown in cyan as α -carbon traces.

dimerization (or oligomerization) of CD4 (15), MHC (18), or TCR (19) as triggering mechanisms.

The structure of unbound human CD4 D1–D4 showed that CD4 molecules form dimers through the D4 domain, at least in the crystal (15). Although it has been suggested that D4–D4-associated CD4 dimers may contribute to T-cell activation by interacting with TCR–pMHC complexes (15, 35), the TCR–pMHC–CD4 structure is incompatible with this idea. First, CD4 is monomeric in the TCR–pMHC–CD4 crystal. Second, in a hypothetical model constructed by superposing the TCR–pMHC–CD4 structure onto the D4–D4-associated CD4 dimer, the vertical distance between the C termini of the D4 domains and the hypothetical T-cell surface is ~ 40 Å, which is too far to be spanned by the short (eight-residue) stalk region of CD4 (Fig. S1). This assembly is, therefore, unlikely to form on the T-cell membrane.

The observation that some HLA-DR molecules crystallize as dimers (18, 36), as well as the detection of MHC class II dimers on cells (37), suggested a mechanism for T-cell triggering whereby an MHC class II dimer cross-links two TCRs. However, the CD4-binding site on HLA-DR4 is nearly coincident with the putative HLA-DR dimerization site (Fig. S2), which would preclude formation of MHC class II dimers, at least through the interface identified in HLA-DR crystals (18, 36).

According to the pseudodimer model of T-cell triggering, one TCR binds an agonist pMHC ligand, whereas a second TCR binds a self-pMHC ligand (14). Dimerization occurs because the CD4 coreceptor associated with the TCR bound to the agonist pMHC complex also interacts with the self-pMHC complex. However, experimental evidence for CD4-mediated TCR cross-linking is lacking. By contrast, it was recently shown that TCRs can dimerize in the cell membrane independently of CD4 and that mutations which impair TCR dimerization also inhibit activation of CD4⁺ T cells (19). Notably, these mutations are located in the C and F strands and AB loop of C α , which form a contiguous surface on the outside of the TCR–pMHC–CD4 arch (Fig. 4C), opposite the site mediating TCR–CD3 interactions (Fig. 4A). As such, CD4 would not interfere sterically with TCR dimerization, nor would it be necessary to displace CD3 subunits to expose the TCR dimerization site in a modified pseudodimer model of T-cell activation (Fig. S3).

CD4 and TCR–pMHC Docking Orientation. Structural studies of >25 TCR–pMHC complexes have demonstrated remarkable similarities in the overall topology of TCR binding to pMHC, irrespective of MHC class I or class II restriction (9, 10). Typically, the TCR docks on pMHC in a central diagonal orientation, with the V α domain over the N-terminal half of the antigenic peptide and the V β domain over the C-terminal half, although the exact angle and pitch of TCR engagement vary. Two competing (although not mutually exclusive) hypotheses have been put forward to explain this roughly conserved diagonal binding mode. The first holds that coevolution of TCR and MHC genes has led to specific interaction motifs between the germline-encoded CDR1 and CDR2 loops of TCRs and the α -helices of MHC proteins (10, 20–22). However, if the interaction of TCR V regions with MHC is governed solely by evolutionarily selected rules, these are not always apparent, even when a particular V region recognizes the same MHC allele (10). According to the second hypothesis, it is the need for coreceptor function during thymic T-cell selection that restricts the geometry of TCR–pMHC recognition and eliminates from positive selection CD4⁺CD8⁺ double-positive thymocytes expressing TCRs unable to engage pMHC in a manner that generates a signal to induce maturation (22–25). In this view, TCR docking topology is guided by the CD4 and CD8 coreceptors during T-cell development to achieve intracellular juxtaposition of coreceptor-bound Lck with CD3 ITAMs.

By establishing anchor points for TCR and CD4 on the T-cell membrane, the TCR–pMHC–CD4 structure imposes constraints on the orientation of CD3 relative to Lck associated with CD4 on the cytoplasmic side of the membrane, thereby providing a framework for understanding how CD4 can focus TCR on MHC to restrict TCR docking options on pMHC. Fig. 5 shows the position of the C terminus of CD4 observed in the complex with TCR MS2-3C8 and HLA-DR4, as well as the predicted position of the C terminus of CD4 in hypothetical ternary complexes constructed using nine other TCR–pMHC class II structures, both human and mouse, assuming that CD4 engages human and mouse MHC class II molecules in the same manner (27). With a single exception, the human autoimmune TCR Ob.1A12 (38), the C termini of CD4 in these modeled complexes form a relatively tight cluster that includes the C terminus of CD4 in the MS2-3C8–MBP–DR4–CD4 complex. Other autoimmune TCRs (3A6, Hy.1B11) also fall within the cluster. The observed variability in the position of the CD4 membrane anchor point is the consequence of variations in the overall diagonal docking topology of the TCR–pMHC structures, which places CD3 ϵ and CD3 δ inside the TCR–pMHC–CD4 arch, opposite CD4 (Fig. 4A). If the TCR–pMHC docking polarity were reversed (i.e., V α over the C terminus of the peptide and V β over the N terminus), we postulate that CD4-bound Lck would be

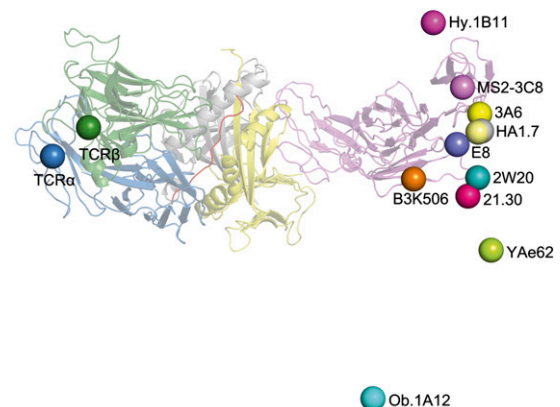


Fig. 5. Orientation of TCR and CD4 in TCR–pMHC–CD4 complexes. Bottom view of the TCR–pMHC–CD4 complex, as if looking up from inside the T cell. TCR α chain, blue; TCR β chain, green; CD4, pink; MHC α chain, gray; MHC β chain, yellow; MBP peptide, red. On the left side of the figure, the C termini of the extracellular portions of the α and β chains of TCR MS2-3C8, as defined in the crystal structure, are indicated by blue and green spheres, respectively. On the right side of the figure, the C terminus of the extracellular portion of CD4 in the complex with MS2-3C8 and HLA-DR4 is marked by a pink sphere labeled MS2-3C8. The right side also shows the predicted position of the C terminus of CD4 in hypothetical ternary complexes constructed using other TCR–pMHC class II structures [human: HA1.7 (PDB ID code 1JH8), Ob.1A12 (PDB ID code 1YMM), 3A6 (PDB ID code 1ZGL), E8 (PDB ID code 2IAM), Hy.1B11 (PDB ID code 3PL6); mouse: B3K506 (PDB ID code 3C5Z), 2W20 (PDB ID code 3C6L), YAe62 (PDB ID code 3C60), 21.30 (PDB ID code 3MBE)]. In each case, the C terminus of CD4 is marked by a colored sphere labeled with the name of the corresponding TCR. The TCR–pMHC–CD4 complexes were modeled by superposing each TCR–pMHC class II structure onto the MS2-3C8–MBP–DR4–CD4 complex through the C domains of the TCRs. In addition, CD4 was assumed to engage mouse MHC class II molecules in the same manner as HLA-DR4, based on the structures of human CD4 D1–D2 bound to mouse I-A^k (12) and of human CD4 D1–D2 bound to HLA-DR1 (27). With the exception of TCR Ob.1A12, the C termini of CD4 in the modeled TCR–pMHC–CD4 complexes form a cluster that includes the C terminus of CD4 in the MS2-3C8–MBP–DR4–CD4 complex. Variability in the position of the CD4 membrane anchor point results from differences in the docking topology of the TCR–pMHC structures. Based on mutational analysis (31, 32), CD3 ϵ and CD3 δ would be located inside the TCR–pMHC–CD4 arch, facing CD4.

impeded from phosphorylating CD3 ITAMs, thus preventing positive selection of T cells bearing those TCRs.

Although the TCR-pMHC-CD8 complex is probably not as conformationally constrained as the TCR-pMHC-CD4 complex, there is evidence that the CD8 stalk may not be as flexible as generally believed, because of *O*-glycosylation at multiple sites in CD8 α and CD8 β (39). Biophysical studies of mucins have shown that *O*-glycans stiffen polypeptides through steric interactions between peptide-linked *N*-acetylgalactosamine residues and adjacent peptide residues (40, 41). Similarly, *O*-glycans in the CD8 stalk polypeptides were found to reduce the overall extension of the stalk from a theoretical maximum of 3.4 Å per residue to 2.6 Å per residue, suggesting rigidification (39, 42). Hence, *O*-glycosylation may limit the mobility of the CD8 head group that binds MHC class I, thereby imposing constraints on the orientation of CD3 relative to CD8-bound Lck, as in the TCR-pMHC-CD4 complex.

At the same time, some flexibility must exist within the overall signaling complex to accommodate variations in TCR-pMHC docking geometry that alter the location of anchor points for TCR and CD4 on the T-cell surface (Fig. 5). Given the relative rigidity of the CD4 ectodomain (Fig. 3), this flexibility most likely resides in interactions involving the cytoplasmic tails of CD3 and CD4 with Lck, which can adopt multiple conformations (43). We conclude that the diagonal docking orientation of $\alpha\beta$ TCRs reflects not only genetically encoded interactions with MHC but also the requirement to form a ternary complex with CD4 or CD8 that is geometrically competent to deliver a maturation signal to double-positive thymocytes during T-cell selection.

Materials and Methods

Protein Production and Purification. Soluble TCR MS2-3C8 and MBP-HLA-DR4 were prepared by *in vitro* folding from inclusion bodies produced in *Escherichia coli* as described (28). For affinity maturation of CD4 by yeast surface display, 12 residues in the D1 domain (positions 35, 40, 42–48, 59, 60, and 63) were mutated by overlap PCR with degenerate primers to generate a CD4 D1–D2 mutant library of 4×10^7 clones (27). The CD4 library was displayed on the surface of yeast by N-terminal fusion to agglutinin protein Aga2p and sorted by flow cytometry with HLA-DR1 tetramers or monomers to isolate CD4 mutants with increased affinity. One of these mutants, containing two substitutions in CD4 D1 (Gln40Tyr/Thr45Trp), was produced as a full-length ectodomain. Thus, CD4 D1–D4 (residues 1–363) was fused to the gp67 secretion signal sequence of baculovirus expression vector pAcGP67-B (BD Biosciences) with a C-terminal FLAG tag (DYKDDDDK) and expressed in Sf9 insect cells (Invitrogen). In a typical preparation, 1 L of Sf9 cells at 1.6×10^6 cells/mL in Sf-900 II SFM medium (Invitrogen) was inoculated with 12 mL of recombinant baculovirus at 4×10^8 pfu/cell. Supernatants were harvested 4 d postinfection and loaded onto an anti-FLAG M2 column (Sigma) for

affinity purification. Recombinant CD4 D1–D4 was eluted with 0.1 mg/mL FLAG peptide and further purified using sequential Superdex S-75 and MonoQ columns (GE Healthcare).

SPR Analysis. The interaction of affinity-matured CD4 with HLA-DR4 was assessed by SPR using a BIAcore T100 biosensor at 25 °C. Biotin-tagged MBP-HLA-DR4 was prepared as described (28) and directionally coupled to a streptavidin-coated BIAcore SA chip. Solutions containing different concentrations of CD4 D1–D4 were injected sequentially over flow cells immobilized with HLA-DR4 or buffer alone as a control. Injections were stopped at 60 s after SPR signals reached a plateau. Equilibrium data were fitted with a 1:1 binding model using BIAevaluation 4.1 software (BIAcore) to obtain the dissociation constant (K_D).

Crystallization and Data Collection. Purified TCR MS2-3C8, MBP-HLA-DR4, and CD4 D1–D4 were mixed in equimolar amounts and concentrated to 13 mg/mL in 10 mM Tris-HCl (pH 8.0), 10 mM sodium acetate (pH 5.2), and 5 mM NaCl. The ternary complex crystallized spontaneously from this protein solution. For data collection, crystals with dimensions up to $0.2 \times 0.1 \times 0.1$ mm were transferred to a cryoprotectant solution containing 25% (wt/vol) polyethylene glycol 4000 and 20% (vol/vol) glycerol, before flash-cooling in liquid nitrogen. X-ray diffraction data were collected to 4.0-Å resolution at beamline 23ID-B of the Advanced Photon Source. The data were indexed, integrated, and scaled with the program CrystalClear (Rigaku). The crystals belong to space group $P4_32_12$ with unit cell dimensions $a = b = 146.2$ Å, $c = 231.4$ Å and one ternary complex molecule per asymmetric unit. Data collection statistics are presented in Table S1.

Structure Determination and Refinement. The structure of the TCR-MHC-CD4 complex was solved by molecular replacement with the program Phaser (44) using MS2-3C8-MBP-DR4 [Protein Data Bank (PDB) ID code 3O6F] (28) and the first three domains (D1–D3) of CD4 (PDB ID code 1WIO) (15) as search models. The D4 domain of CD4 was positioned into the electron density after rigid body refinement of the solution found with CD4 D1–D3. Initial refinement was performed using the deformable elastic network (DEN)-assisted refinement module in CNS v1.3 (45, 46). The model was then manually built in COOT (47) and further refined using PHENIX (48). Refinement statistics are summarized in Table S1. The final R_{work} and R_{free} values (23.8% and 30.5%, respectively) at 4.0-Å resolution compare favorably with statistics for 51 structures deposited in the PDB within the last 3 y with resolutions in the range of 3.9–4.1 Å. The average R_{work} for these structures is 27.8% and average R_{free} is 31.2%.

ACKNOWLEDGMENTS. We are grateful to S. T. Walsh (University of Maryland) for help with X-ray data collection and to M. Mo for assistance with protein expression. We thank Y. Li and L. Deng for comments on the manuscript and R. Martin (University of Zürich) for TCR clones. This work was supported by National Institutes of Health Grants AI036900 and AI073654 and National Multiple Sclerosis Society Grant RG2747 (to R.A.M.). X.X.W. was supported by the Irvington Institute Fellowship Program of the Cancer Research Institute.

- Janeway CA, Jr. (1992) The T cell receptor as a multicomponent signalling machine: CD4/CD8 coreceptors and CD45 in T cell activation. *Annu Rev Immunol* 10:645–674.
- Irvine DJ, Purbhoo MA, Krosggaard M, Davis MM (2002) Direct observation of ligand recognition by T cells. *Nature* 419:845–849.
- Holler PD, Kranz DM (2003) Quantitative analysis of the contribution of TCR/pepMHC affinity and CD8 to T cell activation. *Immunity* 18:255–264.
- Xu H, Littman DR (1993) A kinase-independent function of Lck in potentiating antigen-specific T cell activation. *Cell* 74:633–643.
- Li QJ, et al. (2004) CD4 enhances T cell sensitivity to antigen by coordinating Lck accumulation at the immunological synapse. *Nat Immunol* 5:791–799.
- Artyomov MN, Lis M, Devadas S, Davis MM, Chakraborty AK (2010) CD4 and CD8 binding to MHC molecules primarily acts to enhance Lck delivery. *Proc Natl Acad Sci USA* 107:16916–16921.
- Jiang N, et al. (2011) Two-stage cooperative T cell receptor-peptide major histocompatibility complex-CD8 trimolecular interactions amplify antigen discrimination. *Immunity* 34:13–23.
- van der Merwe PA, Cordoba SP (2011) Late arrival: Recruiting coreceptors to the T cell receptor complex. *Immunity* 34:1–3.
- Rudolph MG, Stanfield RL, Wilson IA (2006) How TCRs bind MHCs, peptides, and coreceptors. *Annu Rev Immunol* 24:419–466.
- Marrack P, Scott-Browne JP, Dai S, Gapin L, Kappler JW (2008) Evolutionarily conserved amino acids that control TCR-MHC interaction. *Annu Rev Immunol* 26:171–203.
- Wucherpfennig KW, Call MJ, Deng L, Mariuzza RA (2009) Structural alterations in peptide-MHC recognition by self-reactive T cell receptors. *Curr Opin Immunol* 21:590–595.
- Wang JH, et al. (2001) Crystal structure of the human CD4 N-terminal two-domain fragment complexed to a class II MHC molecule. *Proc Natl Acad Sci USA* 98:10799–10804.
- Davis SJ, et al. (2003) The nature of molecular recognition by T cells. *Nat Immunol* 4:217–224.
- Krosggaard M, et al. (2005) Agonist/endogenous peptide-MHC heterodimers drive T cell activation and sensitivity. *Nature* 434:238–243.
- Wu H, Kwong PD, Hendrickson WA (1997) Dimeric association and segmental variability in the structure of human CD4. *Nature* 387:527–530.
- Ashish, et al. (2008) Conformational rearrangement within the soluble domains of the CD4 receptor is ligand-specific. *J Biol Chem* 283:2761–2772.
- van der Merwe PA, Dushek O (2011) Mechanisms for T cell receptor triggering. *Nat Rev Immunol* 11:47–55.
- Brown JH, et al. (1993) Three-dimensional structure of the human class II histocompatibility antigen HLA-DR1. *Nature* 364:33–39.
- Kuhns MS, et al. (2010) Evidence for a functional sidedness to the alphabetaTCR. *Proc Natl Acad Sci USA* 107:5094–5099.
- Feng D, Bond CJ, Ely LK, Maynard J, Garcia KC (2007) Structural evidence for a germline-encoded T cell receptor-major histocompatibility complex interaction 'codon'. *Nat Immunol* 8:975–983.
- Scott-Browne JP, White J, Kappler JW, Gapin L, Marrack P (2009) Germline-encoded amino acids in the alphabeta T-cell receptor control thymic selection. *Nature* 458:1043–1046.
- Adams JJ, et al. (2011) T cell receptor signaling is limited by docking geometry to peptide-major histocompatibility complex. *Immunity* 35:681–693.

23. Mazza C, Malissen B (2007) What guides MHC-restricted TCR recognition? *Semin Immunol* 19:225–235.
24. Buslepp J, Wang H, Biddison WE, Appella E, Collins EJ (2003) A correlation between TCR Valpha docking on MHC and CD8 dependence: Implications for T cell selection. *Immunity* 19:595–606.
25. Van Laethem F, et al. (2007) Deletion of CD4 and CD8 coreceptors permits generation of alphabetaT cells that recognize antigens independently of the MHC. *Immunity* 27:735–750.
26. Xiong Y, Kern P, Chang H, Reinherz E (2001) T cell receptor binding to a pMHCII ligand is kinetically distinct from and independent of CD4. *J Biol Chem* 276:5659–5667.
27. Wang XX, et al. (2011) Affinity maturation of human CD4 by yeast surface display and crystal structure of a CD4-HLA-DR1 complex. *Proc Natl Acad Sci USA* 108:15960–15965.
28. Yin Y, Li Y, Kerzic MC, Martin R, Mariuzza RA (2011) Structure of a TCR with high affinity for self-antigen reveals basis for escape from negative selection. *EMBO J* 30:1137–1148.
29. Maekawa A, Schmidt B, Fazekas de St Groth B, Sanejouand YH, Hogg PJ (2006) Evidence for a domain-swapped CD4 dimer as the coreceptor for binding to class II MHC. *J Immunol* 176:6873–6878.
30. Huppa JB, et al. (2010) TCR-peptide-MHC interactions *in situ* show accelerated kinetics and increased affinity. *Nature* 463:963–967.
31. Kuhns MS, Davis MM (2007) Disruption of extracellular interactions impairs T cell receptor-CD3 complex stability and signaling. *Immunity* 26:357–369.
32. Fernandes RA, et al. (2012) The T-cell receptor is a structure capable of initiating signalling in the absence of large conformational rearrangements. *J Biol Chem* 2012 Jan 19 (in press).
33. Xu C, et al. (2008) Regulation of T cell receptor activation by dynamic membrane binding of the CD3 ϵ cytoplasmic tyrosine-based motif. *Cell* 135:702–713.
34. Casasnovas JM, Springer TA, Liu JH, Harrison SC, Wang JH (1997) Crystal structure of ICAM-2 reveals a distinctive integrin recognition surface. *Nature* 387:312–315.
35. Moldovan MC, et al. (2002) CD4 dimers constitute the functional component required for T cell activation. *J Immunol* 169:6261–6268.
36. Ghosh P, Amaya M, Mellins E, Wiley DC (1995) The structure of an intermediate in class II MHC maturation: CLIP bound to HLA-DR3. *Nature* 378:457–462.
37. Cherry RJ, et al. (1998) Detection of dimers of dimers of human leukocyte antigen (HLA)-DR on the surface of living cells by single-particle fluorescence imaging. *J Cell Biol* 140:71–79.
38. Hahn M, Nicholson MJ, Pyrdol J, Wucherpfennig KW (2005) Unconventional topology of self peptide-major histocompatibility complex binding by a human autoimmune T cell receptor. *Nat Immunol* 6:490–496.
39. Shore DA, Wilson IA, Dwek RA, Rudd PM (2005) Glycosylation and the function of the T cell co-receptor CD8. *Adv Exp Med Biol* 564:71–84.
40. Shogren R, Gerken TA, Jentoft N (1989) Role of glycosylation on the conformation and chain dimensions of O-linked glycoproteins: Light-scattering studies of ovine submaxillary mucin. *Biochemistry* 28:5525–5536.
41. Gerken TA, Butenhof KJ, Shogren R (1989) Effects of glycosylation on the conformation and dynamics of O-linked glycoproteins: Carbon-13 NMR studies of ovine submaxillary mucin. *Biochemistry* 28:5536–5543.
42. Merry AH, et al. (2003) O-glycan sialylation and the structure of the stalk-like region of the T cell co-receptor CD8. *J Biol Chem* 278:27119–27128.
43. Boggon TJ, Eck MJ (2004) Structure and regulation of Src family kinases. *Oncogene* 23:7918–7927.
44. Storoni LC, McCoy AJ, Read RJ (2004) Likelihood-enhanced fast rotation functions. *Acta Crystallogr D Biol Crystallogr* 60:432–438.
45. Brünger AT, et al. (1998) Crystallography & NMR system: A new software suite for macromolecular structure determination. *Acta Crystallogr D Biol Crystallogr* 54:905–921.
46. Schröder GF, Levitt M, Brünger AT (2010) Super-resolution biomolecular crystallography with low-resolution data. *Nature* 464:1218–1222.
47. Emsley P, Lohkamp B, Scott WG, Cowtan K (2010) Features and development of Coot. *Acta Crystallogr D Biol Crystallogr* 66:486–501.
48. Adams PD, et al. (2010) PHENIX: A comprehensive Python-based system for macromolecular structure solution. *Acta Crystallogr D Biol Crystallogr* 66:213–221.